

Complex history of the Rembrandt basin and scarp system, Mercury

Sabrina Ferrari (sabrina.ferrari@studenti.unipd.it) (1), Matteo Massironi (1,2), Christian Klimczak (3), Paul K. Byrne (3), Gabriele Cremonese (4) and Sean C. Solomon (3). (1) Department of Geosciences, University of Padua, Padova, Italy, (2) CISAS, University of Padua, Padova, Italy, (3) Department of Terrestrial Magnetism, Carnegie Institution of Washington, Washington DC 20015, USA, (4) Astronomical Observatory of Padua, INAF, Padova, Italy.

1. Introduction

During its second and third flybys, the MESSENGER spacecraft [1] imaged the well-preserved Rembrandt basin in Mercury's southern hemisphere. With a diameter of 715 km, Rembrandt is the second largest impact structure recognized on Mercury after the 1550-km-diameter Caloris basin. Rembrandt is also one of the youngest major basins [2] and formed near the end of the Late Heavy Bombardment (~3.8 Ga). Much of the basin interior has been resurfaced by smooth, high-reflectance units interpreted to be of volcanic origin [3]. These units host sets of contractional and extensional landforms generally oriented in directions radial or concentric to the basin, similar to those observed within the Caloris basin [4-6]; these structures are probably products of multiple episodes of deformation [2,7,8].

Of particular note in the Rembrandt area is a 1,000-km-long reverse fault system [9] that cuts the basin at its western rim and bends eastward toward the north, tapering into the impact material. On the basis of its shape, the structure has previously been characterized as a lobate scarp. Its formation and localization have been attributed to the global contraction of Mercury [2].

From MESSENGER flyby and orbital images, we have identified previously unrecognized kinematic indicators of strike-slip motion along the Rembrandt scarp, together with evidence of interaction between the scarp orientation and the concentric basin-related structural pattern described above. Here we show through cross-cutting relationships and scarp morphology that the development of the Rembrandt scarp was strongly influenced by tectonics related to basin formation and evolution.

2. Mapping of the Rembrandt area

Through morphological and structural analysis of Mercury Dual Imaging System (MDIS) images at different spatial resolutions, combined with stereo-derived topography [10], we created a geological map of the Rembrandt area (Fig. 1).

On the basis of spectral and textural properties of the surface, we subdivided the Rembrandt basin into three main units: (1) the *Hummocky Area*, a mixture of impact melt and breccias that in places has been reworked by smaller impacts; this unit is mainly confined along the northern part of the basin (Fig. 1); (2) the *Proximal Ejecta*, present just outside the basin rim (Fig. 1); this unit formed during the Rembrandt impact event and thus is coeval with the hummocky material; and (3) the volcanic *Inner Plains*, which flooded the crater floor (Fig. 1) after the impact and can be distinguished in sub-units through color variations (which we interpret as indicators of differences in composition, maturity, or both).

From structural mapping, we distinguish between global-scale and basin-localized structures (Fig. 1). The Rembrandt scarp, as the main global structure, represents the surface expression of a large-scale thrust fault that verges toward the south (outside the basin) to southeast (inside the basin). The thrust is accompanied by a gentle back-thrust and displays kinematic indicators of lateral shearing. We divide the Rembrandt scarp into two parts, on the basis of these lateral kinematic indicators: the portion of the scarp outside the basin shows clear evidence of right-lateral strike slip movement whereas that portion inside the basin shows some evidence of a left-lateral component.

3. Discussion

Unlike smaller lobate scarps elsewhere on the planet, the Rembrandt scarp shows unusual structural and morphological characteristics, including the abrupt change in strike direction, the contrasting lateral shearing indicators [11,12], and marked differences in scarp elevation outside and inside Rembrandt basin. We interpret this suite of features as evidence that the basin had a fundamental role in the development of the scarp. This influence could have been active or passive, depending on the relative time of the basin-forming impact event.

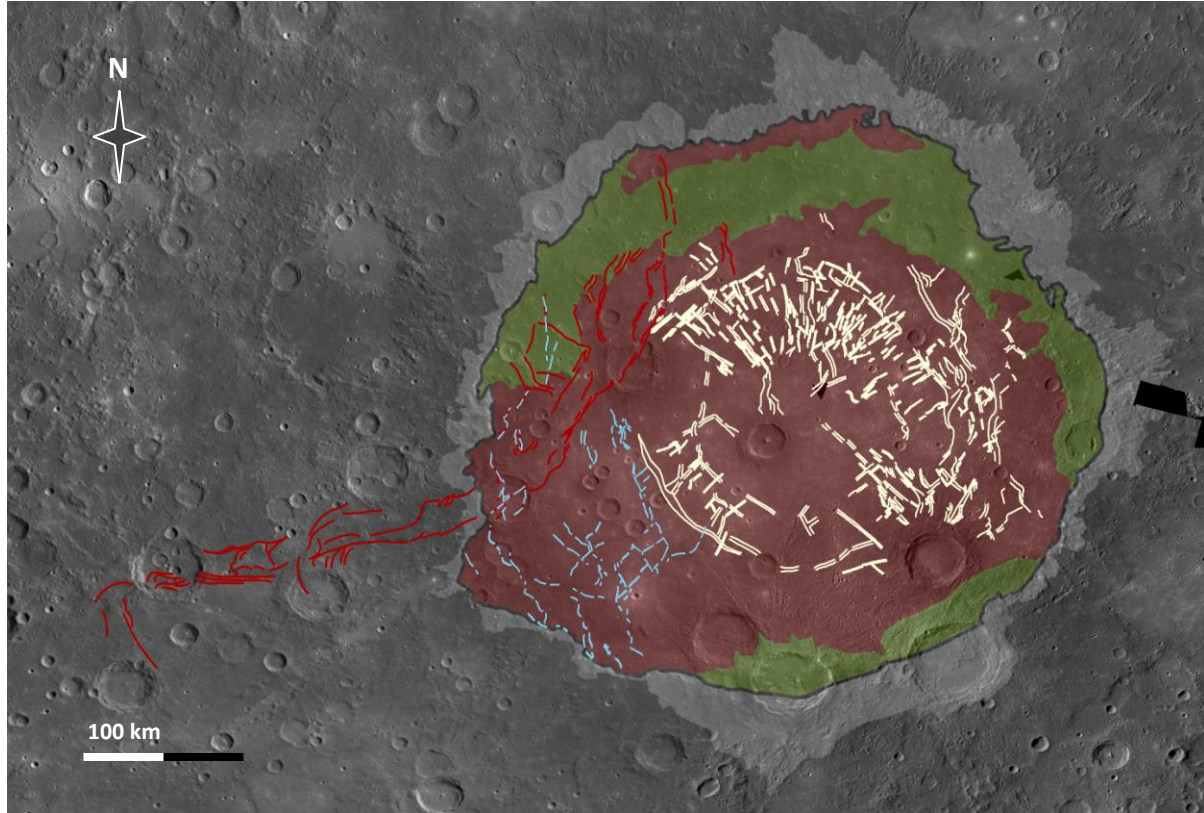


Fig. 1: Geological map of the Rembrandt basin and scarp system centered at 33°S, 81°E, on a MESSENGER MDIS mosaic at 250 m/px. Hummocky Area (green unit); Proximal Ejecta (pale grey unit); Inner Plains (red unit); Rembrandt scarp reverse fault system (red lines); basin-related structures (white lines); secondary features of uncertain origin (blue lines).

If the impact came before initiation of thrust faulting, it probably led to the generation of basin-related structures and an inhomogeneous crustal layering that passively influenced the development and final geometry of the scarp. On the other hand, if the impact event occurred during activity along the thrust, it could have led to a substantial change in the (regional) stress field as well as a local reworking of the structure. These effects could have induced changes in scarp vergence, the appearance of later strike-slip structures, and passive control of basin structures on scarp evolution.

4. Conclusion

The morphological and structural interpretation of MESSENGER flyby and orbital images (Fig. 1) and topography [10] has allowed us to study complex relationships between the Rembrandt basin and its through-going scarp. In particular, we find strong evidence for interaction between Rembrandt basin-

scale and regional-scale stress fields, which have acted to influence the orientation and kinematic development of the Rembrandt scarp. Future analysis will focus on determining the sequence of formation for these features, i.e., whether the scarp predates or postdates the basin.

References

- [1] S. C. Solomon et al. (2008) *Science*, 321, 59. [2] T. R. Watters et al. (2009) *Science*, 324, 618. [3] B. W. Denevi et al. (2009) *Science*, 324, 613. [4] S. L. Murchie et al. (2008) *Science*, 321, 73. [5] T. R. Watters et al. (2009) *EPSL*, 285, 283. [6] P. K. Byrne et al. (2012) *LPS*, 43, 1722. [7] R. G. Strom (1972) *Mod. Geol.*, 2, 133. [8] T. R. Watters et al. (2005) *Geology*, 33, 669. [9] P. K. Byrne et al. (2012) *LPS*, 43, 2118. [10] F. Preusker et al. (2011) *PSS*, 59, 1910. [11] S. Ferrari et al. (2011) *EPSC-DPS*, 963. [12] M. Massironi et al. (2012) *LPS*, 43, 1924.